Terminal Short Arm Domains of Basement Membrane Laminin Are Critical for Its Self-assembly

Johannes C. Schittny and Peter D. Yurchenco

Department of Pathology, Robert Wood Johnson Medical School, Piscataway, New Jersey 08854-5635

Abstract. Laminin self-assembles into large polymers by a cooperative two-step calcium-dependent mechanism (Yurchenco, P. D., E. C. Tsilibary, A. S. Charonis, and H. Furthmayr. 1985. *J. Biol. Chem.* 260:7636–7644). The domain specificity of this process was investigated using defined proteolytically generated fragments corresponding to the NH_2-terminal globule and adjacent stem of the short arm of the B1 chain (E4), a complex of the two short arms of the A and B2 chains attached to the proximal stem of a third short arm (E1′), a similar complex lacking the globular domains (P1′), and the distal half of the long arm attached to the adjacent portion of the large globule (E8). Polymerization, followed by an increase of turbidity at 360 nm in neutral isotonic TBS containing $CaCl_2$ at 35°C, was quantitatively inhibited in a concentration-dependent manner with laminin fragments E4 and E1′ but not with fragments E8 and P1′. Affinity retardation chromatography was used for further characterization of the binding of laminin domains. The migration of fragment E4, but not of fragments E8 and P1′, was retarded in a temperature- and calcium-dependent fashion on a laminin affinity column but not on a similar BSA column. These data are evidence that laminin fragments E4 and E1′ possess essential terminal binding domains for the self-aggregation of laminin, while fragments E8 and P1′ do not. Furthermore, the individual domain-specific interactions that contribute to assembly are calcium dependent and of low affinity.

BASEMENT membrane laminin is a multidomain glycoprotein composed of three polypeptide chains in a four-armed structure (4). The NH_2-terminal moieties of the B1, B2, and A chains form the three short arms of laminin, each containing multiple cysteine-rich repeats (domains III and V) and pairs of globular domains (domains IV and VI). The sequence of the A chain (19) indicates it also possesses a third short arm globule, a structure difficult to detect by electron microscopy. These three chains join at the intersection of the cross, fusing to form a long (77-nm) alpha-helical triple coiled-coiled arm (16) and a terminal globular domain, the latter exclusively formed by the A chain (19). This glycoprotein is a major structural component of basement membranes and interacts with both cells and structural macromolecules. The interactions contributing to cell binding or basement membrane architecture involve specific regions or domains of laminin. Entactin (nidogen), a dumbbell-shaped glycoprotein, tightly binds the inner cross region of laminin (17). This protein in turn serves to bridge laminin to type IV collagen (21). Type IV collagen also appears to bind directly to the ends of the long and short arms (3). Heparin and related glycosaminoglycans bind the long arm globule of laminin (14). Finally, laminin binds to itself.

Laminin self-assembly is characterized by the formation of large polymers (26). The process appears to occur by nucleation/propagation and can be divided into two steps. The first step is temperature dependent, with the formation of small oligomers in which both long and short arm terminal interactions can be visualized by electron microscopy. In the second step, oligomers are converted to large aggregates: this step requires the presence of divalent cations, especially calcium (26). At a concentration >2 μM, laminin undergoes a sol-to-gel transition (27). While the supramolecular organization of laminin in tissue has not yet been determined through direct visualization, there is indirect evidence to support the hypothesis that a laminin polymer exists also in vivo. First, laminin can be found in basement membrane (13 μM in Engelbreth-Holm-Swarm tumor matrix), well above both the sol-to-gel transition point and the minimum concentration that would allow each molecule to bind its laminin neighbor (25). Second, most laminin can be liberated in soluble form from various basement membranes simply by the addition of EDTA or EGTA to neutral isotonic buffer (17). Third, there are laminin-rich basement membranes that lack a type IV collagen scaffolding (1). Recently, it has been found (15) that each laminin can bind ~16 calcium ions, that calcium appears to induce conformational changes in the protein (18), and that one to two of these interactions are of sufficient affinity to account for laminin polymerization.

In this study, we have examined the domain specificity and the temperature and calcium dependence of the self-assembly reaction of the protein domains contained in fragments E4, E8, E1′, and P1′.

Materials and Methods

Preparation and Labeling of Laminin and Its Fragments

Laminin. Purification steps were carried out at 0–5°C. Laminin was isolated from lathyritic Engelbreth-Holm-Swarm tumor as the laminin-entactin complex based on the method of Paulsson et al. (17). While entactin (nidogen) is not required for laminin self-assembly (15), the laminin-entactin complex purified in this fashion gave more reproducible results with respect to quantitation of polymer formed. Briefly, ~250 g of frozen tumor was homogenized in 0.1 M NaCl, 50 mM Tris-HCl, pH 7.4, containing 0.5 mM diisopropyl fluorophosphate, 10 μg/ml p-hydroxymercuribenzoate, and 1 mM PMSF. After washing the pellet by centrifugation, laminin-entactin was twice extracted with 500 ml of the above buffer containing 10 mM EDTA and centrifuged to remove insoluble residue. Aliquots (100 ml) of combined extract were chromatographed on a Sephacryl S500 (Pharmacia Fine Chemicals, Uppsala, Sweden) column (5 × 95 cm) in 0.1 M NaCl, 50 mM Tris-HCl, pH 7.4, 2.5 mM EDTA, 10 μg/ml p-hydroxymercuribenzoate, 1 mM PMSF. The first and major peak was then pooled and loaded onto a DEAE-Sephacel (Pharmacia Fine Chemicals) column (5 × 10 cm) equilibrated in 50 mM Tris-HCl, pH 7.4, 2.5 mM EDTA, 10 μg/ml p-hydroxymercuribenzoate, 1 mM PMSF. After collection of an unbound fraction of laminin-entactin, the column was subjected to an 0–0.8 M linear NaCl gradient (total 1 l). The unbound and first bound peak were separately pooled. The unbound and bound fractions were used for the experiments or the generation of defined proteolytic fragments, as described below.

Preparation of Laminin Fragments E1′, E4, and E8. The elastase fragments were generated proteolytically and purified by a modification of the methods of Ott et al. (14) and Paulsson et al. (18). Laminin-entactin, at ~2 mg/ml in TBS (0.13 M NaCl, 10 mM Tris-HCl, pH 7.4) with 2 mM EDTA, was digested with a 1:240 enzyme-to-substrate ratio with porcine elastase (Serva Fine Biochemicals Inc., Garden City Park, NY; 101 U/mg) at 4°C for 1 h and then 25°C for 23 h. After inhibiting further digestion with 1 mM PMSF, aliquots (15–20 ml) of digested protein were loaded onto a Sepharose CL-6B column (2.6 × 90 cm) and eluted with the same buffer. Four peaks were obtained, the second usually as a shoulder on the first: the first was enriched in E1′, the second in E8, and the third in E4. These peaks were pooled, dialyzed into 50 mM Tris-HCl, 0.5 mM PMSF, pH 8.5, concentrated with Aquacide (Calbiochem-Behring Corp., San Diego, CA), and purified by ion exchange high performance liquid chromatography on a glass-packed TSK-DEAE-5PW column (0.8 × 7.5 cm; LKB Instruments, Inc., Gaithersburg, MD), which was eluted with an 0–0.5 M NaCl gradient in the same buffer. Purity was assayed by SDS-PAGE and electron microscopy of rotary-shadowed Pt/C replicas.

Preparation of Laminin Fragment P1′. As previously described (26) laminin-entactin was dialyzed into 10% acetic acid and digested with pepsin (Sigma Chemical Co., St. Louis, MO) at an enzyme-to-substrate ratio of 1:15 and a laminin concentration of 0.9 mg/ml at 15°C for 24 h. The reaction was stopped by adjusting the pH to 7.4 with 1 N NaOH. The protein was then dialyzed into 50 mM Tris-HCl, 1 mM PMSF, pH 7.4, concentrated with Aquacide II (Calbiochem-Behring Corp.) to ~20 ml, and mixed with $CaCl_2$ to a final concentration of 1 M. Final purification was accomplished by gel filtration on a 2.5 × 95-cm agarose A-5m (Bio-Rad Laboratories, Richmond, CA) in 50 mM Tris, pH 7.4, containing 1 M $CaCl_2$ and 1 mM PMSF.

Radioiodination of Laminin Fragments. 1 mg of laminin fragment E8 was dialyzed into TBS and mixed with 1–2 mCi of carrier-free $Na^{125}I$ (ICN Radiochemicals, Irvine, CA), 20 μl of a 1 mg/ml solution of lactoperoxidase (Sigma Chemical Co.), and 50 μl of 0.003% hydrogen peroxide. The sample was incubated at 22–26°C for 15–20 min, placed on ice, and mixed with 50 μl of saturated aqueous tyrosine. The solution was then purified on a 2-ml (~10 × 0.6-cm) Sephadex G-25 column (Pharmacia Fine Chemicals) and equilibrated in TBS with 0.2 mM EDTA to remove the bulk of free iodine. The pooled peak was then further purified by gel filtration in the cold on an 0.6 × 45-cm Sepharose CL-6B column. Samples, after pooling, were stored as aliquots in liquid nitrogen.

1 mg each of laminin fragments E4 and P1′ were dialyzed into 0.13 M NaCl, 10 mM sodium phosphate, pH 7.4, and added to 400 μCi of ^{125}I-Bolton-Hunter reagent (NEM Research Products, Boston, MA). The solutions were incubated on ice for 2 h. The reaction was stopped with 20 μl of 0.5 M glycine in TBS for 30 min. The samples were then purified on separate 2-ml Sephadex G-25 columns (Pharmacia Fine Chemicals) and, in a second step in the cold, on separate 0.6 × 45-cm Sepharose CL-6B columns, all equilibrated in TBS containing 2.5 mM EDTA, 10 μg/ml p-hydroxymercuribenzoate, 1 mM PMSF.

Analytical Techniques

Turbidity Assay. Laminin was dialyzed into TBS containing 1 mM $CaCl_2$ and centrifuged in 1–1.5-ml aliquots at 40,000 rpm at 2°C in a type 65 rotor (Beckman Instruments, Inc., Fullerton, CA) for 70 min. The supernatants were used for turbidity and centrifugation assays. Laminin self-aggregation was followed by the increase of turbidity at 360 nm in TBS containing 1 mM $CaCl_2$ at 35°C for 60 min. Samples were placed in prewarmed 1-ml quartz cuvettes, and absorbance was measured at 1-min intervals in an automated double beam spectrophotometer (model Lambda-4; Perkin-Elmer Corp., Oceanport, NJ) using a buffer blank. The self-aggregation of laminin was inhibited, using constant laminin (0.25 mg/ml) but increasing fragment concentrations (0–1.6 mg/ml). It was found that the fragments themselves, incubated without laminin, produced no measurable turbidity. The percentage of inhibition was calculated setting the increase of turbidity of the pure laminin samples as 100%.

Sedimentation Assay. Samples with constant ^{125}I-laminin (0.25 mg/ml, 35,000–50,000 cpm/mg), but variable fragment concentration (0–1.6 mg/ml), were incubated in TBS, 1 mM $CaCl_2$ at 35°C for 60 min in quartz cuvettes or 1.5-ml Eppendorf tubes and were spun at 13,500 rpm (16,000 *g*) using these tubes in a Hermle (Goshaim, West Germany) Z231M microcentrifuge. The laminin concentration was determined in the supernatant at the beginning of the incubation and after centrifugation. The degree of inhibition was calculated by comparing the sedimented protein of a pure laminin sample (100%) with the samples containing laminin and defined fragments.

Affinity Retardation Chromatography. The migration of different fragments on a long laminin affinity column (3 mm × 35 cm) relative to that on a similar BSA column (3 mm × 35 cm) was compared. The proteins were coupled to AffiGel 15 (Bio-Rad Laboratories) in 0.1 M Hepes (Sigma Chemical Co.). The final columns contained 1.25 mg laminin or 1.7 mg BSA per 1 ml gel, respectively. During the chromatograph, two or three drop fractions were taken and either the counts of ^{125}I-labeled fragments or the protein concentration of the fractions were followed (protein assay kit; Bio-Rad Laboratories). The void volume of both columns was determined using blue dextran 2000 (Sigma Chemical Co.) and laminin fragment P1′, which both appeared at the same position. The total volume was determined for every chromatography using phenol red or free ^{125}I radioactivity. To compare the relative elution positions between columns, K_{av} was defined as $(V_e - V_o)/V_t - V_o)$, where V_e is the elution volume, V_o is the void volume, and V_t is the total volume. K_{av} is dependent on both the affinity between the column and the fragment and on the sizing effect of the gel to which the protein was coupled.

SDS-PAGE. SDS-PAGE was carried out on 3.5–12% linear gradient gels, as described (10), and gels were stained with Coomassie brilliant blue R250.

Electron Microscopy. Macromolecular samples (15–40 μg/ml) in 55% glycerol, 45% 0.15–0.2 M ammonium bicarbonate were sprayed onto freshly cleaved mica and rotary shadowed at an 8° angle with 0.6–0.8 nm Pt/C in a BAF 301 or 500 freeze-etch-fracture unit (Balzers, Hudson, NH) (20). Replicas were examined in a 420 electron microscope (Philips Electronic Instruments, Inc., Mahwah, NJ) at 60 kV with a 30-μm objective aperture.

Results

Laminin Fragments

Defined fragments of laminin (elastase fragments E1′, E4, and E8 and pepsin fragment P1′) were used to investigate the self-binding of laminin (Fig. 1). E1′ is observed in rotary-shadowed Pt/C replicas as a Y-shaped particle with two short (each ~37-nm-long) arms, each with a pair of globules and a third shorter arm segment (~20 nm), the latter lacking the inner globular domain (Fig. 2 *b*). Occasionally an additional small stub is observed on one of its arms. When analyzed by SDS-PAGE, the fragment migrates as a doublet (460/420 kD) nonreduced and several bands if reduced, indicating that the complex is held together by internal disulfides (Fig. 2 *a*). Fragment E4, which is the NH_2-terminal end (domains VI and V) (7) of the B1 chain short arm, has the appearance of a small globule and stem in Pt/C replicas (Fig. 2 *e*) and migrates by SDS-PAGE reduced and unreduced as a single band

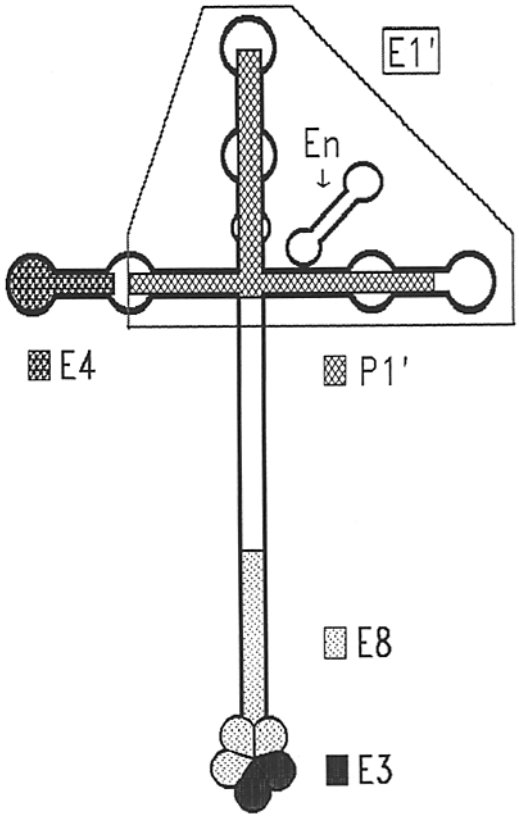

Figure 1. Domain structure of laminin. Localization of the elastase fragment E1′, E4, E3, and E8 and the pepsin fragment P1′ within the four-arm structure of laminin and an approximate position of the dumbbell-shaped entactin (nidogen) molecule (*En*) in the laminin–entactin complex.

of apparent relative molecular mass of 75 kD (Fig. 2 *a*). Fragment E8 is the distal stem and proximal half of the large globule of the long arm of laminin. In rotary-shadowed replicas, it is seen as a thin rod connected to a globule (Fig. 2 *d*) and migrates as two bands by SDS-PAGE, the larger band at 120 kD and the smaller band at ~80 kD (nonreduced) and smaller when reduced (Fig. 2 *a*). Recently, it has been reported (2) that fragment E3, which represents subdomains G4 and G5 of the A chain, is adjacent to and not included in the globular domain of fragment E8. Fragment P1′ is produced after pepsin digestion: morphologically it is seen as a Y-shaped particle with one arm ~35 nm long and the other two arms 20–25 nm long, all without recognizable globules. Like E1′, it is a short arm complex but lacks the intact globular domains (Fig. 2 *c*). In nonreduced SDS–polyacrylamide gels, it migrates with an apparent relative molecular mass of 350 kD, smaller than E1′ (Fig. 2 *a*).

Inhibition of the Laminin Polymerization

Laminin–entactin aggregated in a typical sigmoidal fashion as measured by turbidity at 35°C TBS containing 1 mM $CaCl_2$ (26). The increase of turbidity could be inhibited with laminin fragments E4 and E1′ but not with fragments P1′ and E8 or with BSA (Fig. 3). Previously, it has been shown that there is a linear relationship between the amount of polymer and turbidity (26). However, since we did not know whether this relationship would remain linear in the presence of inhibition fragments, the amount of polymer formed at different inhibiting concentrations of fragment was also directly quantitated by sedimentation. The inhibition of laminin aggregation was dependent on the concentrations of fragments E4 and E1′, with 50% inhibition achieved at a 3-fold

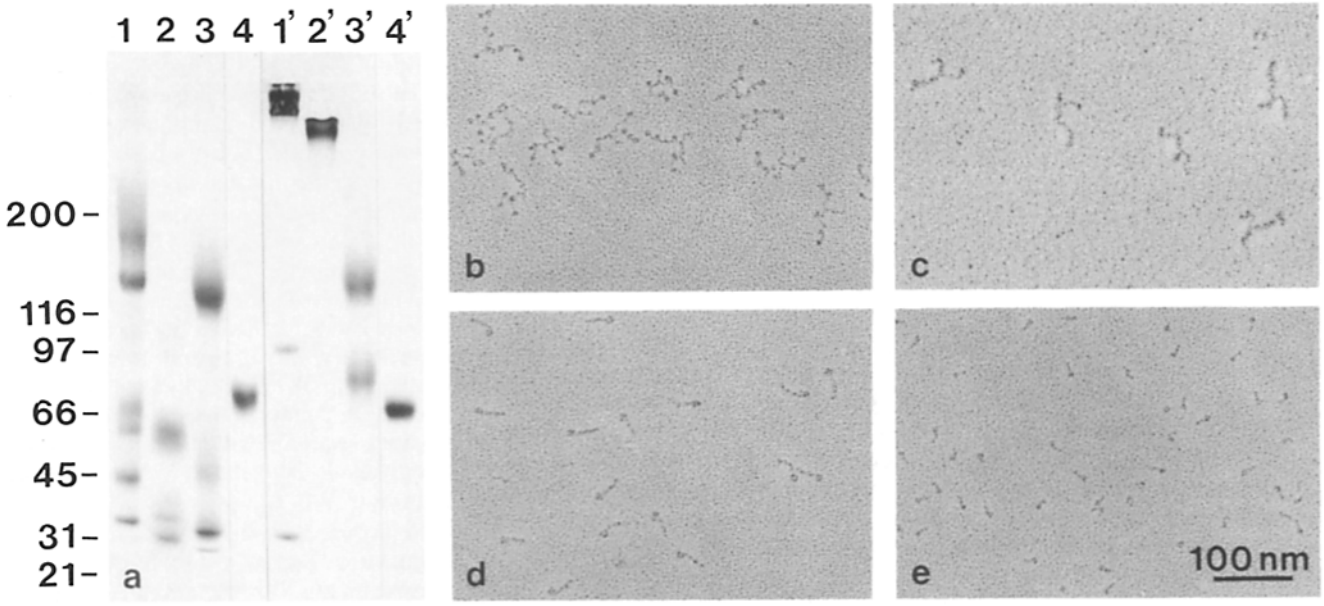

Figure 2. Laminin fragments. (*a*) SDS-PAGE of laminin fragments. Electrophoresis was performed in 3.5–12% gradient gels with (lanes *1–4*) and without prior reduction (lanes *1′-4′*). Samples were fragments E1′ (lanes *1* and *1′*), P1 (lanes *2* and *2′*), E8 (lanes *3* and *3′*), and E4 (lanes *4* and *4′*). The position of standard proteins of known relative molecular mass are indicated. (*b–e*) Rotary shadowing electron microscopy of laminin fragments. Representative electron micrographs of laminin fragments E1′ (*b*), P1′ (*c*), E8 (*d*), and E4 (*e*) after low angle rotary shadowing with Pt/C. Bar, 100 nm.

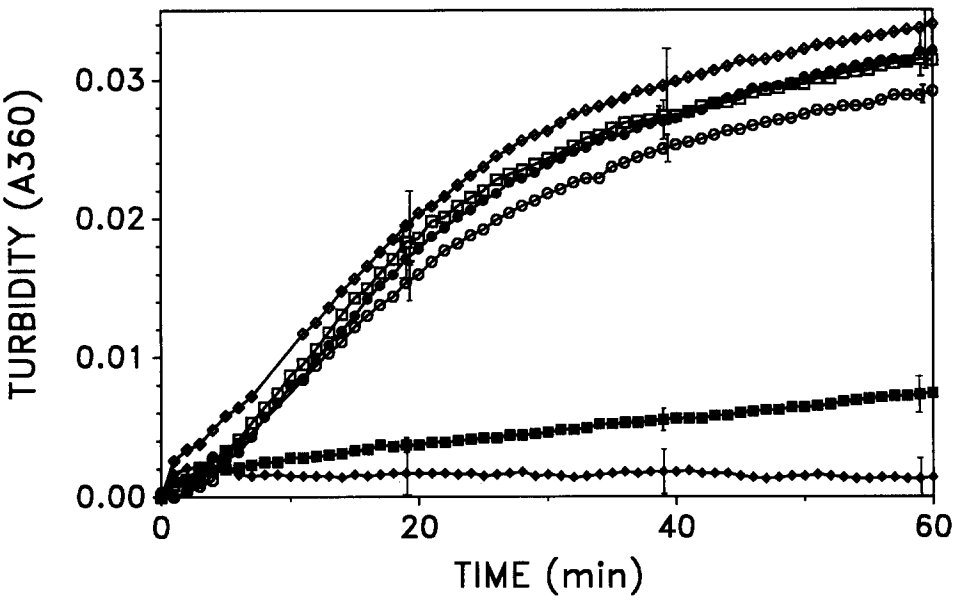

Figure 3. Time course of an inhibition of the laminin polymerization. Laminin self-aggregation was followed by the increase of turbidity at 360 nm in TBS containing 1 mM calcium at 35°C (*solid circle*). Elastase fragments E4 (*solid square*; 0.125 mg/ml) and E1′ (*solid diamond*; 0.8 mg/ml) inhibited laminin self-assembly in contrast to fragments E8 (*open circle*; 0.48 mg/ml) and P1′ (*open diamond*; 0.56 mg/ml) and BSA (*open square*; 0.115 mg/ml). The laminin–entactin concentration of all samples was 0.25 mg/ml and the molar ratio of laminin to inhibitor was 1:8 (0.21:1.7 μM). Every data point represents the mean of three or four parallel processed samples. The standard deviation is shown for every twentieth data point.

(E1′) to 5-fold (E4) molar excess and essentially complete inhibition achieved at a 30-fold molar excess of fragment (Fig. 4). In contrast, fragments E8 and P1′ as well as BSA failed to show any effect on the laminin aggregation, even at high concentrations (16–32-fold molar excess; Fig. 4). The results of the centrifugation assay correlated well with the inhibition of turbidity.

The molecular morphology of laminin-fragment mixtures was examined. Laminin (0.25 mg/ml) was incubated either alone or in molar excess of E4 (0.2 mg/ml) or P1′ (0.1–0.4 mg/ml) for 30 min at 35°C in TBS, 0.1 mM $CaCl_2$, diluted 20-fold into ammonium bicarbonate, glycerol, rotary shadowed, and examined in the electron microscope. The striking finding was that, while many large laminin polymer aggregates were noted in the laminin and laminin–P1′ preparations, mostly free monomers, scattered oligomeric forms, and only rare aggregates were observed with a laminin–E4 mixture. The laminin–E4 replicas, however, were less useful for determination of binding specificity. First, obvious interactions were not frequently observed. Second, most apparent interactions were ambiguous with respect to binding location. We would attribute the first problem to mass action dissociation for a relatively low affinity interaction after dilution (see below) and the second to the difficulty in discerning a small particle adjacent to a large flexible macromolecule.

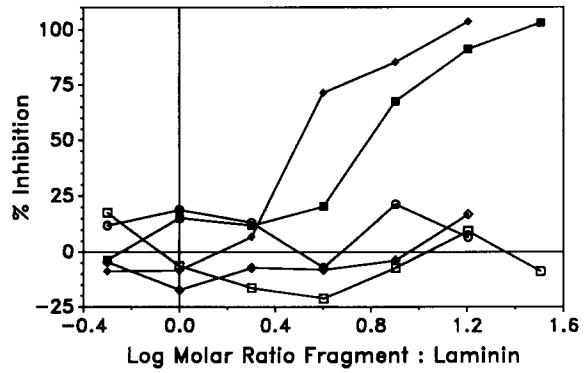

Figure 4. Concentration dependency of the inhibition of the laminin polymerization. The inhibition of the laminin self-aggregation was followed by the centrifugation assay. ^{125}I-laminin (0.25 mg/ml) and variable amounts of unlabeled fragments were incubated in TBS containing 1 mM calcium at 35°C. The aggregates were sedimented, and the amount of the formed polymer was determined by the measurement of the ^{125}I-laminin concentration in the supernatant. The percentage of inhibition is dependent on the concentration of fragment E4 (*solid square*; 0.008–0.5 mg/ml) and E1′ (*solid diamond*; 0.05–1.6 mg/ml). In contrast, even 16–32-fold molar excess of the fragments E8 (*open circle*; 0.03–0.96 mg/ml) and P1′ (*open diamond*; 0.03–1.12 mg/ml) or of BSA (*open square*; 0.007–0.46 mg/ml) failed to interfere with the laminin polymerization. In the absence of inhibitors, 70% of the total laminin aggregated and precipitated.

Affinity Retardation Chromatography

While overall affinities for cooperative protein polymerization can be substantial, individual domain interactions that contribute to self-assembly are often of low affinity (13). This turned out to be the case with laminin and required the development of a detection method that limits dissociation during separation of bound from unbound species. We first evaluated the method of equilibrium gel filtration (8). However, this method proved to be unsatisfactory because most of the laminin became trapped inside the column. Therefore, we instead took advantage of the ability of ligands to be retarded in their migration down a long specific binding column when the affinities are not sufficiently high to permit complete immobilization. In buffer conditions of physiological ionic strength and pH, the migration of different laminin fragments was determined on specific affinity columns. Retardation of migration, as determined against a standard nonreacting (reference) column, was used as a measure of relative affinity. This relative retardation on the affinity column is caused by a shifting of the distribution between the stationary and the mobile phase towards the stationary phase. The first (affinity) column was prepared by covalently coupling laminin (as the laminin–entactin complex) to the gel. The second

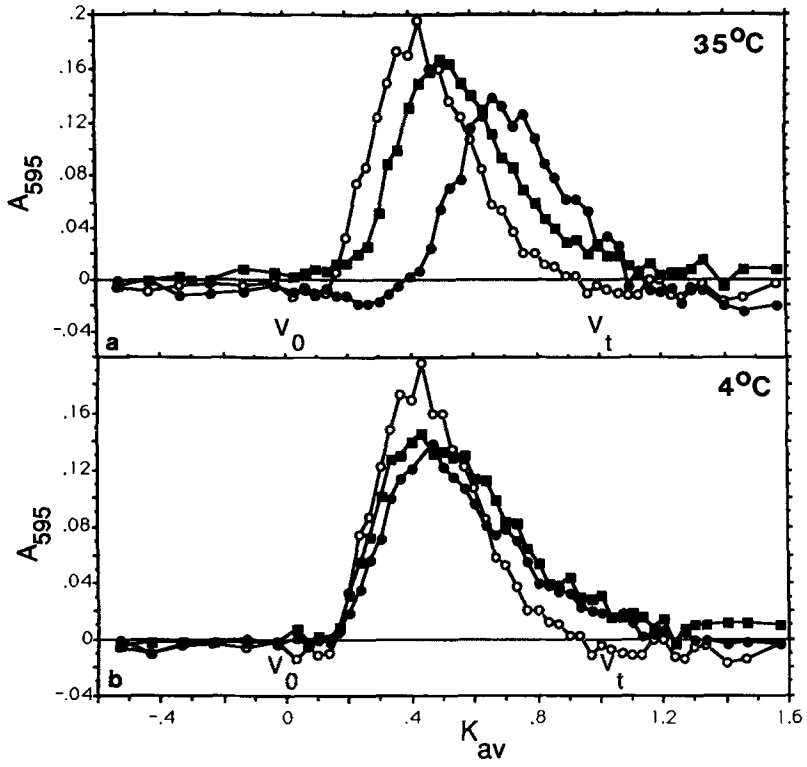

Figure 5. Affinity retardation chromatography of fragment E4. (*a*) The migration behavior of fragment E4 on a BSA affinity column (*open circle*) and on a similar laminin column (*solid circle*) in TBS containing 1 mM $CaCl_2$ at 35°C was evaluated. Relative to the BSA column a substantial retardation could be detected on the laminin column. Under the same conditions, except that the buffer contains 1 mM EDTA instead of calcium, the retardation on the laminin column appears to be in between that on the BSA column and that on the laminin column with calcium present (*solid square*). (*b*) At 4°C, no difference in the migration of fragment E4 could be detected between the BSA (*open circle*) and the laminin column, independent of whether calcium (*solid circle*) or EDTA (*solid square*) was present in the buffer. The protein concentration in each fraction was determined using the Bradford assay and measuring the optical density at 595 nm. K_{av} is the position relative to the void (zero; V_o) and the total volume (one; V_t) of the column.

and third (reference) columns were coupled with BSA or laminin fragment PI′, respectively. The void volume of every column was determined using laminin fragment PI′ and the fastest moving peak of blue dextran (both gave the same value). The total (included) volume was determined with phenol red and free ^{125}I and was used to normalize migration and the peak positions for each column. K_{av} was defined as the relative peak position on a column, setting the void volume as zero and the total volume as one. Because the migration is dependent on the molecular sieve effect of the gel and the binding affinity between the immobilized and the mobile ligand, the elution volume could be larger than the total volume of the column. Therefore, K_{av}, as used here, may be larger than one. The migration of the fragments E4, PI′, and E8 were compared on different Affigel 15 columns coupled to no protein (water), laminin, BSA, or fragment PI′ under nonbinding conditions (1 mM EDTA, 4°C). No difference in the sieving characteristics for each of these components on the four columns could be detected. Therefore, it appears unlikely that the sieving properties are affected by the protein coupling. The fractionation range of these columns was determined to be ~5–2,000 kD. We refer to this method, which represents modifications of a basic approach used for nonproteinaceous ligands (5, 9), as affinity retardation chromatography.

At 35°C, the migration of the fragment E4 was retarded (Fig. 5 *a*) on the laminin affinity column relative to that on a reference column of identical dimensions but coupled to albumin. Retardation, and hence binding affinity, of E4 was calcium dependent. In buffer containing 1 mM $CaCl_2$, the retardation of fragment E4 on the laminin column was the greatest. Its K_{av} value was shifted from 0.43 on the BSA

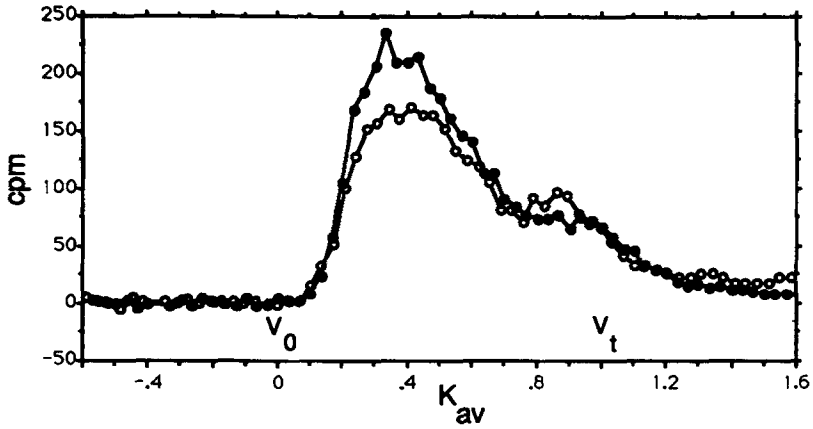

Figure 6. Affinity retardation chromatography of fragment E8. The retardation of ^{125}I-labeled fragment E8 on a laminin column (*solid circle*) was compared with the behavior on a similar BSA affinity column (*open circle*) in TBS containing 1 mM $CaCl_2$ at 35°C. No difference could be detected. The small peak in the total volume of the BSA and laminin column is due to free counts (see results). K_{av} is the position relative to the void (zero; V_o) and the total volume (one; V_t) of the column.

column to 0.66 on the laminin column. In calcium-depleted buffer (1 mM EDTA), E4 retardation was significantly less, and the K_{av} shifted only from 0.43 on the BSA column to 0.50 on the laminin column. Thus, binding of E4 to laminin is decreased if calcium is absent. The binding of E4 was also found to be temperature dependent (Fig. 5 *b*). In contrast to 35°C, no significant retardation or binding, respectively, could be detected at 4°C either with or without calcium (K_{av} values = 0.43–0.45).

For fragment E8, no binding to laminin could be detected (Fig. 6). This fragment migrated at a position of K_{av} equal to 0.34–0.36 on the laminin, BSA, and fragment P1′ affinity columns in TBS with or without calcium and at 4 or 35°C (plot for 35°C and 1 mM calcium shown [plot not shown for other conditions]; the small peak in the total volume of the BSA and laminin column is due to free counts because the peak contains no protein and appears at the same position as free iodine). As a further control, the interaction of fragment P1′ with laminin was investigated because it was expected from previous studies (26) that this fragment would not bind to laminin or to itself. Fragment P1′ migrated very consistently at the same position (K_{av} = 0.16) on the three affinity columns regardless of which buffer or temperature was used (plots for 35°C and 1 mM calcium shown in Fig. 7).

The affinity retardation behavior of fragment E1′ was also examined. In calcium-containing TBS, fragment E1′ became trapped on both the laminin affinity (laminin) and the reference (BSA) column and could not be eluted unless high salt, EDTA-containing TBS (1 M NaCl, 1 mM EDTA), was used. In calcium-depleted buffer (TBS, 1 mM EDTA), no trapping or retardation occurred. It appeared likely that this trapping effect was a consequence of E1′ self-interactions similar to the effect encountered earlier with intact laminin. To pursue the oligomerization effect further, the E1′ complexes were visualized in rotary-shadowed replicas after exchange from TBS containing 1 mM calcium into 0.2 M ammonium bicarbonate (Fig. 8). The electron micrographs revealed the presence of small to intermediate-sized oligomers. These complexes were smaller than the aggregates produced by intact laminin, and no large polymers were observed. The later finding is consistent with the result that fragment E1′ does not cause any turbidity if incubated under laminin polymerization conditions (TBS, 1 mM $CaCl_2$, 35°C). Like earlier observations for intact laminin (26), in many cases end-to-end interactions of fragment E1′ were observed, but often the structure was too complex to interpret in an unambiguous manner.

Discussion

Laminin self-assembly has the characteristics of a cooperative nucleation/propagation assembly: there is a critical concentration (~60 μM) below which aggregation does not occur and there is a relative paucity of oligomeric intermediates in incubation mixtures (26). Assembly can be divided into a temperature-dependent oligomer step and a calcium-dependent polymer step. Polymerization is thermally reversible, and laminin can be cycled between an aggregated and nonaggregated state by cycling between 35 and 0–5°C. While it is not clear if calcium plays a regulatory role in vivo (e.g., to inhibit laminin self-assembly before its release into the extracellular space) or if the role of calcium is simply to stabilize laminin constitutively into a functional conformation, the divalent cation effect has helped to dissect the polymerization process.

When the polymerization of laminin (26) was first described, the main evidence for domain specificity was the electron microscopic identification of oligomers with end-to-end associations. The presence of additional or different interactions among the large polymers could not be excluded in electron micrographs of low angle-shadowed preparations. From our study of the polymerization-inhibiting properties and direct binding capabilities of defined laminin fragments, it is now possible to substantiate a number of these earlier findings as well as to extend our understanding of the complex set of specific interactions that contribute to polymerization.

By measuring the increase of laminin turbidity or sedimented aggregates, we have shown that laminin polymerization can be quantitatively inhibited with fragment E4, which possesses the NH_2-terminal short arm globular domain from the B1 chain (7), and with fragment E1′, which possesses the NH_2-terminal globular domain pairs of the A and the B2 chain. In contrast, fragment P1′, which lacks the terminal domains of the short arms, and fragment E8 do not possess the ability to interfere with the laminin polymerization (Figs. 1, 3, and 4). Paulsson et al. (18) have shown by a combination of cross-linking and gel filtration in chaotropic buffers that fragment E1′ forms small oligomers in the presence of cal-

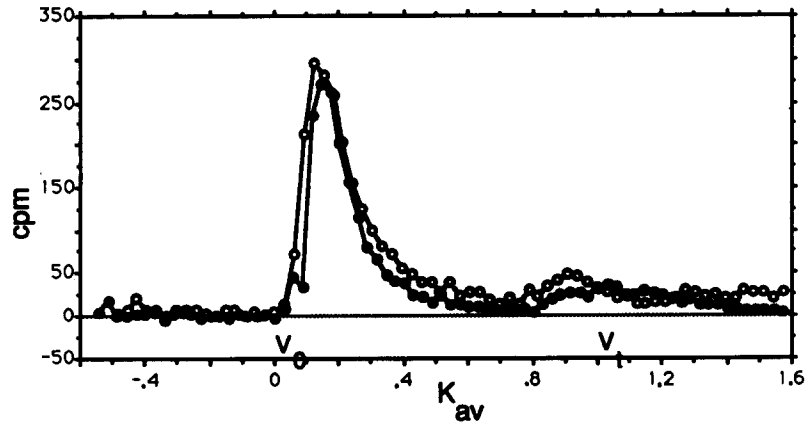

Figure 7. Affinity retardation chromatography of fragment P1′. Comparing the migration of ^{125}I-labeled fragment P1′ on a BSA affinity column (*open circle*) and on a laminin affinity column (*solid circle*), no difference could be detected in TBS containing 1 mM $CaCl_2$ at 35°C. Therefore, no binding of fragment P1′ to laminin was observed. K_{av} is the position relative to the void (zero; V_o) and the total volume (one; V_t) of the column.

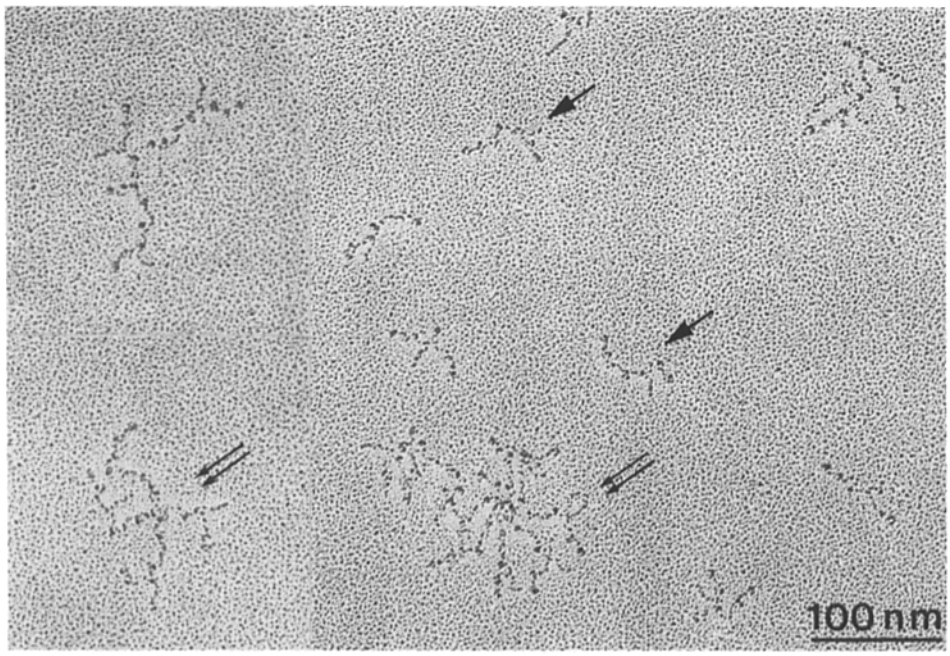

Figure 8. Electron micrograph of rotary-shadowed replica of fragment E1′. Fragment E1′ maintained in TBS containing 1 mM calcium was dialyzed into 0.2 M ammonium bicarbonate, sprayed onto mica, and rotary shadowed at low angle with Pt/C. Monomeric E1′ (*arrows*) as well as small-to-medium-sized E1′ oligomers (*double arrows*) were observed. End-to-end interactions of fragment E1′ can be identified, whereas additional binding sites can not be excluded in more complex aggregates.

cium, while smaller fragments like E1 have lost this ability. Our results are in agreement with their findings. Fragment E1′ was visualized by electron microscopy and monomeric and oligomeric forms were observed (Fig. 8). At 35°C with calcium present, fragment E1′ was trapped in our columns, a consequence, we believe, of the formation of E1′ complexes. Fragment P1′, on the other hand, neither binds to laminin nor forms oligomers. Therefore, we conclude that the NH_2-terminal globular domains of the short arms are critical for self-assembly. The visualization of end-to-end interaction in fragment E1′ oligomers is consistent with this interpretation. However, additional binding sites cannot be excluded because the structure of the oligomers was often too complex to decipher. Recently, Bruch et al. (2) generated a larger fragment (designated C1-4), consisting of all three intact short arms, with cathepsin G. Like intact laminin, this fragment forms large aggregates in calcium-containing buffers. The principal difference between the large cathepsin fragment and fragment E1′ is that the former possesses the terminal globule found in E4. Collectively, these data provide evidence that the self-aggregation domains of the short arms are most likely located in their terminal regions and that the intactness of the three short arms is critical for the laminin polymerization.

Previously, it has been found that half-maximal laminin aggregation is achieved at ~10 μM Ca^{2+} with one to two calcium interactions of sufficient affinity to account for the development of conformational changes that confer polymerization activity (15, 18). Using affinity retardation chromatography, the temperature and calcium dependency of domain E4 binding was studied. The binding of fragment E4 to laminin shows the same temperature and calcium dependency as observed for laminin self-assembly (Fig. 5). We do not fully understand which domain contains the one or two calcium binding sites necessary for the polymerization. However, we conclude that fragment E1′ possesses at least one of these sites since calcium is required for fragment E1′ self-aggregation (18) or binding to laminin.

What is the structural role of laminin in basement membranes? One view of basement membrane organization is that type IV collagen forms the only polymeric scaffolding which then serves as a binding locus for all other basement membrane proteins (6, 11, 24). This would appear unlikely since there are laminin-rich basement membranes that lack type IV collagen (1). The observation that laminin can form large polymers on its own using domain-specific interactions argues for a double polymer system in basement membranes possessing both type IV collagen and laminin. Laminin could contribute to basement membrane architecture through specific terminal arm interactions. The fixed arm lengths and the specific interactions between the end of the arms would produce a specific geometry in three-dimensional space. This geometry would probably not be rigid because each individual molecule exhibits some degree of flexibility. The spatial relationships between the laminin and the collagen IV polymers may then be maintained through direct laminin-to-collagen binding (probably of low affinity) (3) and indirectly through an entactin (nidogen) bridge (22).

During development (12, 24), laminin is laid down as the first abundant basement membrane protein and, during angiogenesis, it is the first one to be observed at the growing tip of a new capillary (6). Here, laminin may provide the only polymer scaffolding and may be the predecessor to a more stable laminin–collagen network. While the type IV collagen network becomes rapidly covalently cross-linked after assembly, the laminin polymer is, initially at least, held together by a number of noncovalent and low affinity, but specific, interactions. Such a laminin–polymer-based matrix has the potential to be remodeled through readily reversible interactions, a feature we would expect to be useful in a developing basement membrane. This ability to dissociate appears to be lost in a number of basement membranes after

development and with aging. Placental laminin, for example, is difficult to extract without the aid of proteolysis (23), whereas laminin is easily dissociated with EDTA in isotonic buffer from embryonic Reichert's membrane or from the Engelbreth-Holm-Swarm tumor (tumor matrix and its laminin are only a few weeks old at time of harvest). Laminin polymer gels, stored at 35°C over several weeks, lose their ability to dissociate even if during storage no covalent bonds are formed. This observation may be the in vitro counterpart to the above-mentioned findings in placenta. Thus, the early plasticity and reversibility of laminin supramolecular architecture may give way to a stable and relatively irreversible assembly no longer subject to remodeling. This structural transition needs to now be considered in the context of the specific domain interactions described in this study.

This work was supported by grant Ro1-DK36425 from the National Institutes of Health. Johannes C. Schittny is a fellow of the Deutsche Forschungsgemeinschaft.

Received for publication 9 August 1989 and in revised form 8 November 1989.

References

1. Brauer, P. R., and J. M. Kelle. 1989. Ultrastructure of a model basement membrane lacking type IV collagen. *Anat. Rec.* 223:376–383.
2. Bruch, M., R. Landwehr, and J. Engel. 1990. Dissection of laminin by cathepsin G into its long arm and short arm structures and localization of regions involved in calcium-dependent stabilization and self-association. *Eur. J. Biochem.* In press.
3. Charonis, A. S., E. C. Tsilibary, P. D. Yurchenco, and H. Furthmayr. 1985. Binding of laminin to type IV collagen: a morphological study. *J. Cell Biol.* 100:1848–1853.
4. Engel, J., E. Odermatt, and A. Engel. 1981. Shapes, domain organizations and flexibility of laminin and fibronectin, two multifunctional proteins of the extracellular matrix. *J. Mol. Biol.* 150:97–120.
5. Fassina, G., and I. M. Chaiken. 1987. Analytical high-performance affinity chromatography. *In* Advances in Chromatography. J. C. Giddings, E. Grushka, and P. R. Brown, editors. Marcel Dekker, Inc., New York. 27:247–297.
6. From, D. M., B. M. Pratt, and J. A. Madri. 1986. Endothelial cell proliferation during angiogenesis: in vitro modulation by basement membrane components. *Lab. Invest.* 55:521–530.
7. Fujiwara, S., H. Shinkai, R. Deutzmann, M. Paulsson, and R. Timpl. 1988. Structure and distribution of N-linked oligosaccharide chains on various domains of mouse tumour laminin. *Biochem. J.* 252:453–461.
8. Hummel, J. P., and W. J. Dryer. 1962. Measurement of protein-binding phenomena by gel filtration. *Biochim. Biophys. Acta.* 63:532–534.
9. Inman, J. K. 1983. A study of multispecific interactions by quantitative affinity chromatography. *In* Affinity Chromatography and Biological Recognition. I. M. Chaiken, M. Wilchek, and I. Parikh, editors. Academic Press, Inc., Orlando, FL. 153–163.
10. Laemmli, U. K. 1970. Cleavage of structural proteins during the assembly of the head of bacteriophage T4. *Nature (Lond.).* 227:680–685.
11. Laurie, G. W., J. T. Bing, H. K. Kleinman, J. R. Hassell, M. Aumailley, G. R. Martin, and R. J. Feldmann. 1986. Localization of binding sites from laminin, heparan sulfate proteoglycan and fibronectin on basement membrane (type IV) collagen. *J. Mol. Biol.* 189:205–216.
12. Leivo, I., A. Vaheri, R. Timpl, and J. Wartiovaara. 1980. Appearance and distribution of collagens and laminin in the early mouse embryo. *Dev. Biol.* 76:100–114.
13. Oosawa, F., and S. Asakura. 1975. Thermodynamics of the polymerization of protein. Academic Press, Inc., New York. 199 pp.
14. Ott, U., E. Odermatt, J. Engel, H. Furthmayr, and R. Timpl. 1982. Protease resistance and conformation of laminin. *Eur. J. Biochem.* 123: 63–72.
15. Paulsson, M. 1988. The role of Ca^{2+} binding in the self-aggregation of laminin–nidogen complexes. *J. Biol. Chem.* 263:5425–5430.
16. Paulsson, M., R. Deutzmann, R. Timpl, D. Dalzoppo, E. Odermatt, and J. Engel. 1985. Evidence for coiled-coil alpha-helical regions in the long arm of laminin. *EMBO (Eur. Mol. Biol. Organ.) J.* 4:309–316.
17. Paulsson, M., M. Aumailley, R. Deutzmann, R. Timpl, K. Beck, and J. Engel. 1987. Laminin–nidogen complex: extraction with chelating agents and structural characterization. *Eur. J. Biochem.* 166:11–16.
18. Paulsson, M., K. Saladin, and R. Landwehr. 1988. Binding of Ca^{2+} influences susceptibility of laminin to proteolytic digestion and interactions between domain-specific laminin fragments. *Eur. J. Biochem.* 177:477–481.
19. Sasaki, M., H. K. Kleinman, H. Huber, R. Deutzmann, and Y. Yamada. 1988. Laminin, a multidomain protein: the A chain has a unique globular domain and homology with the basement membrane proteoglycan and the laminin B chains. *J. Biol. Chem.* 263:16536–16544.
20. Shotten, D. M., B. E. Burke, and D. Branton. 1979. The molecular structure of human erythrocyte spectrin: biophysical and electron microscopic studies. *J. Mol. Biol.* 131:303–329.
21. Timpl, R. 1989. Structure and biology of the laminin–nidogen complex. *Springer Ser. Biophys.* 3:92–101.
22. Timpl, R. 1989. Structure and biological activity of basement membrane proteins. *Eur. J. Biochem.* 180:487–502.
23. Wewar, U., R. Alberchtsen, M. Manthorpe, S. Varon, E. Engvall, and E. Ruoslahti. 1983. Human laminin isolated in a nearly intact, biological active form from placenta by limited proteolysis. *J. Biol. Chem.* 258: 12654–12660.
24. Wu, T. C., Y. J. Wan, A. E. Chung, and I. Damjanov. 1983. Immunohistochemical localization of entactin and laminin in mouse embryos and fetuses. *Dev. Biol.* 100:496–505.
25. Yurchenco, P. D. 1990. Assembly of basement membranes. *Ann. NY Acad. Sci.* In press.
26. Yurchenco, P. D., E. C. Tsilibary, A. S. Charonis, and H. Furthmayr. 1985. Laminin polymerization in vitro: evidence for a two-step assembly with domain specificity. *J. Biol. Chem.* 260:7636–7644.
27. Yurchenco, P. D., Y. S. Cheng, and J. C. Schittny. 1990. Heparin modulation of laminin polymerization. *J. Biol. Chem.* In press.